Journal of Rock Mechanics and Geotechnical Engineering xxx (2015) 1–9

Contents lists available at ScienceDirect

Journal of Rock Mechanics and Geotechnical Engineering

journal homepage: www.rockgeotech.org

Full length article

Load eccentricity effects on behavior of circular footings reinforced with geogrid sheets

Ehsan Badakhshan*, Ali Noorzad

Faculty of Civil, Water & Environmental Engineering, Shahid Beheshti University, Tehran, Iran

ARTICLE INFO

Article history:
Received 11 May 2015
Received in revised form
9 August 2015
Accepted 12 August 2015
Available online xxx

Keywords:
Model test
Circular footing
Eccentric load
Reinforced sand
Bearing capacity

ABSTRACT

In this paper, an experimental study for an eccentrically loaded circular footing, resting on a geogrid reinforced sand bed, is performed. To achieve this aim, the steel model footing of 120 mm in diameter and sand in relative density of 60% are used. Also, the effects of depth of first and second geogrid layers and number of reinforcement layers (1–4) on the settlement-load response and tilt of footing under various load eccentricities (0 cm, 0.75 cm, 1.5 cm, 2.25 cm and 3 cm) are investigated. Test results indicate that ultimate bearing capacity increases in comparison with unreinforced condition. It is observed that when the reinforcements are placed in the optimum embedment depth ($u/D = 0.42$ and $h/D = 0.42$), the bearing capacity ratio (*BCR*) increases with increasing load eccentricity to the core boundary of footing, and that with further increase of load eccentricity, the *BCR* decreases. Besides, the tilt of footing increases linearly with increasing settlement. Finally, by reinforcing the sand bed, the tilt of footing decreases at 2 layers of reinforcement and then increases by increasing the number of reinforcement layers.

1. Introduction

In civil engineering, most of foundations, especially foundations with industrial application, are subjected to horizontally seismic and wind forces, in addition to vertical forces that cause eccentric loading. It is reported by several researchers that the eccentric loading reduces the soil bearing capacity (e.g. Eastwood, 1955; Dhillon, 1961; Graudet and Kerisel, 1965; Lee, 1965; Michalowski and You, 1998; Mahiyar and Patel, 2000; Taiebat and Carter, 2002). Meyerhof (1953) reported that when a strip or rectangular foundation is subjected to an eccentric load, the contact pressure decreases linearly from toe to heel, and subsequently proposed the concept of effective width. Prakash and Saran (1971) provided a comprehensive mathematical formulation to estimate ultimate bearing capacity and settlement for strip foundations in a cohesive soil subjected to eccentric loading. Purkayastha and Char (1977) proposed a reduction factor method for continuous foundations supported by sand. For high silos, refinery towers, wind turbines and chimneys, circular foundation is more economical than any other form of footing, and this is because direction of overturning from wind and earthquake is not fixed and load eccentricity always occurs in one way.

In the case of circular foundations under eccentric loading, Highter and Anders (1985) provided a graphical solution to determine the effective area. The effective area is defined as an equivalent area of footing which can be loaded centrally when a vertical load is applied at a location other than the centroid of footing or when a foundation is subjected to a centric load and momentum. Moreover, Meyerhof (1953) and Vesic (1973) suggested an equation to calculate the effective area in circular footing. In the last four decades, geosynthetics application has been known as a common technique to increase the ultimate bearing capacity of soils and decrease the settlement of footing. Yetimuglu et al. (1994), Adams and Collin (1997), Alawaji (2001), Ghosh et al. (2005), Kumar et al. (2007), Mosallanezhad et al. (2008), Latha and Somwanshi (2009), Vinod et al. (2009), and Moghaddas Tafreshi and Dawson (2010) reported when the reinforcements are placed in the optimum depth from the surface of footing (strip, square, rectangular foundations), the maximum beneficial effect of reinforcement can be achieved. However, few researches have been carried out in the field of sand or clay reinforced with geosynthetic layers. These researches have considered centrically loaded circular foundations in comparison with other foundations.

Boushehrian and Hataf (2003) found that, for the circular footings on reinforced sand, the maximum bearing capacity occurs at different values of embedment depth ratio depending on the number of reinforcement layers N and that, for the ratio of u/D (u is the embedment depth of first layer of reinforcement, and D is the diameter of circular footing) greater than one, reinforcement layers

* Corresponding author. Tel.: +98 126595684.
E-mail address: E_Badakhshan@sbu.ac.ir (E. Badakhshan).

Peer review under responsibility of Institute of Rock and Soil Mechanics, Chinese Academy of Sciences.
1674-7755
http://dx.doi.org/10.1016/j.jrmge.2015.08.006

Please cite this article in press as: Badakhshan E, Noorzad A, Load eccentricity effects on behavior of circular footings reinforced with geogrid sheets, Journal of Rock Mechanics and Geotechnical Engineering (2015), http://dx.doi.org/10.1016/j.jrmge.2015.08.006

have no significant effect on bearing capacity. They also explained that choosing a rigid reinforcement does not always lead to a better effect on bearing capacity. Basudhar et al. (2007) carried out a numerical analysis to study the behavior of circular footings with different sizes resting on reinforced sand with geotextile, and found that with an increase in number of reinforcement layers, the settlement gradually decreases at a decreasing rate. Lovisa et al. (2010) studied the behavior of prestressed geotextile reinforced sand bed supporting a loaded circular footing. They found that the effect of the prestressed geotextile configuration is evident in greater footing depths in comparison with unreinforced and reinforced sand beds without prestressed counterparts.

Regarding loading with eccentricity, only few studies were performed experimentally to identify the critical values of reinforcement layers for reinforcing the soil under strip and rectangular foundations. Sawwaf (2009) conducted a series of model tests on eccentrically loaded strip footing resting on geogrid reinforced sand, and found that the effect of reinforcement on bearing capacity ratio is greater at lower values of eccentricity and greater relative densities. They figured out that the maximum improvement occurs at a depth ratio of $u/B = 0.33$ and $h/B = 0.5$ (B is the width of footing, and h is the vertical distance between reinforcement layers).

Furthermore, Patra et al. (2006) proposed an empirical relationship from model loading tests on an eccentrically loaded strip foundation in geogrid reinforced sand bed. Sadoglu et al. (2009) reported that the reinforcement increases ultimate loads in comparison with unreinforced cases, and this contribution becomes much lower with increasing load eccentricity. Al-Tirkity and Al-Taay (2012) showed that, for the strip footings, the optimum values of u/B for the first geogrid layer vary from 0.35 to 0.45 depending on the value of load eccentricity.

The experimental studies mentioned above focused on eccentrically loaded strip footing resting on reinforced soil, and no attention was paid to the behavior of eccentrically loaded circular foundation resting on reinforced sand. The present study focuses on the effects of different parameters of geogrid layers, such as the depth of first and second layers of reinforcement, number of reinforcement layers, on the bearing capacity, settlement and tilt of the circular footing resting on sand bed under different load eccentricities.

2. Materials properties

To investigate the effect of eccentric loading on a circular footing resting on reinforced sand with geogrid layers, the properties of materials used in the tests are described in this section.

2.1. Sand

In this study, the poorly graded medium sand dried by the oven is used. The particle size distribution curve, as shown in Fig. 1, is determined using the dry sieving method according to the standard of ASTM D422-90 (1990) on two sand samples. The sand is classified as SP (poorly graded sand) in the unified soil classification system (USCS) with a coefficient of uniformity (C_u) of 2.89, a coefficient of curvature (C_c) of 1.05, and an effective size (D_{10}) of 0.27 mm. In order to determine the specific gravity of soil particles, the maximum and minimum dry densities, the maximum and minimum void ratios, three types of tests are carried out and average values for the sand are computed to be 2.65, 1.64 g/cm^3, 1.44 g/cm^3, 0.89 and 0.65, respectively. The angle of internal friction of dry sand with relative density of 60% is 39°, which is determined by the direct shear test.

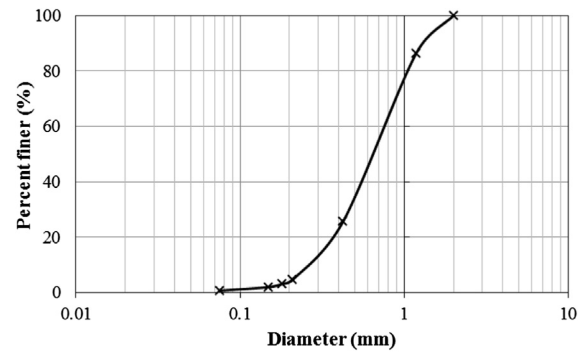

Fig. 1. Particle size distribution curve for the sand.

2.2. Geogrid

In order to provide reinforcement material for the model test, geogrid CE121 with tensile strength of 7.68 kN/m is used. This geogrid has an oval shaped aperture (with 6 mm small diameter and 8 mm large diameter) and is made of high-density polyethylene (HDPE). The reason for selection of this type of geogrid is that the peak tensile strengths in every direction are identical. The physico-mechanical properties of this geogrid categorized in both medium and stiff types are listed in Table 1.

2.3. Footing

The model circular footing is made of steel plates in 15 mm thickness to provide the rigid footing condition. The diameter of footing is selected as 120 mm. The base of footing is roughened by gluing a layer of geogrid on the bottom of circular footing with epoxy glue to ensure uniform roughness in all the tests. To prepare different eccentricities on the footing, several holes are considered for loading and the footing is allowed to rotate freely. The load eccentricity for the footing is chosen according to the core of circular footing, which is a part of footing where the whole footing undergoes compressive pressure when load is applied on other places, except for the center, and when load is applied on the core boundary, the edge of footing has zero pressure. The core of circular footing is computed to be $R/4$ which is equal to 1.5 cm, as given below:

$$q = 0 \Rightarrow q = \frac{P}{A'} - \frac{My}{I} = 0 \Rightarrow \frac{P}{\pi R^2} = \frac{PeR}{\frac{\pi R^4}{4}} \Rightarrow e = \frac{R}{4} \tag{1}$$

where q is the pressure at the edge of the footing, P is the centric load, A' is the area of footing, M is the moment, y is the maximum

Table 1
Physico-mechanical properties of geogrid.

Geogrid name	Aperture shape	Opening size (mm × mm)	Mesh thickness (mm)	Tensile strength (kN m^{-1})	Extension at 1/2 peak load (%)	Extension at maximum load (%)	Tensile strength at 10% extension (kN m^{-1})	Mass per unit area (g m^{-2})
CE121	Oval	6 × 8	3.3	7.68	3.2	20.2	6.8	730

distance from the center, I is the moment of inertia, e is the load eccentricity, and R is the radius of circular footing. In the present study, five load eccentricities are assumed, i.e. centric ($e = 0$), inside of the core ($e = 0.75$ cm), on the core boundary ($e = 1.5$ cm), outside the core ($e = 2.25$ cm) and further away from the core ($e = 3$ cm). The core of footing and loaded locations are demonstrated in Fig. 2.

3. Test apparatus, program and setup

The tests are conducted using the apparatus with a square tank with inside dimensions of 0.6 m × 0.6 m × 0.6 m in length, width and height, respectively. Tank dimensions are 5 times longer than the diameter of footing to ensure that the footing rupture occurs inside the tank. Finally, displacements are measured by the linear variable differential transducer (LVDT).

In all tests, the unit weight and relative density of sand are 15.14 kN/m^3 and 60%, respectively. Pouring technique is used to achieve the desired relative density. The height of free pouring is obtained through several trials in an especial aluminum cup with certain volume of 130 mL. Afterwards, it is found that the tank should be filled in 50 mm thickness interval in order to obtain the desired density. The tank is filled up until the depth of the sand reaches to 50 cm (about 4.2 times the diameter of footing). Meanwhile, a cup pouring the sand with a certain volume is placed in the tank and, after each test, the relative density of sand in the cup is calculated as a sample of the tank soil. The variation of sand relative density is found to be (60 ± 4)% in all tests. In the reinforced cases, a square shaped geogrid layer with the width of 4.5 times the diameter of footing ($L/D = 4.5$, L is the width of reinforcement layer) is placed after leveling the sand surface and this selection is made based on previous researches (Sitharam and Sireesh, 2004; Basudhar et al., 2007; Latha and Somwanshi, 2009), and sand pouring is continued to the selected surface of footing. After preparation of sand in the soil tank, the final level of the sand is flattened from center of the tank into the sides by a steel ruler and extra soil mass is removed without disturbance. Then the circular footing is placed and the head of loading rod is put on the footing. Two LVDTs, with an accuracy of 0.01 mm, are used in all tests: one on the footing surface and the other in the loading place. By determining the difference between the two LVDTs and measuring the distance between them, we are able to calculate the tilt of

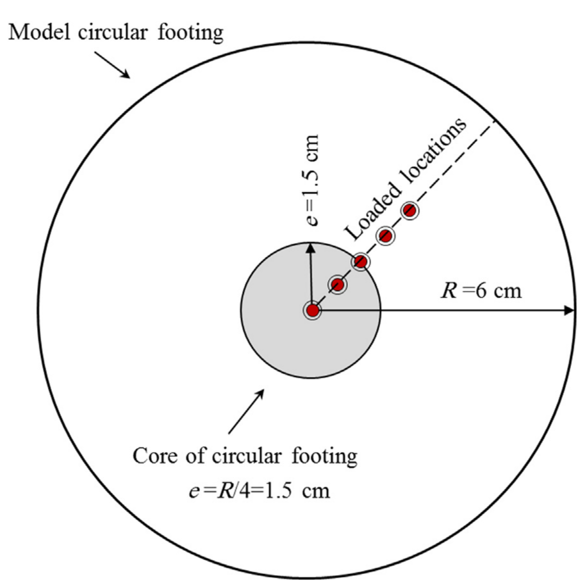

Fig. 2. The core of footing for circular foundation and loaded locations.

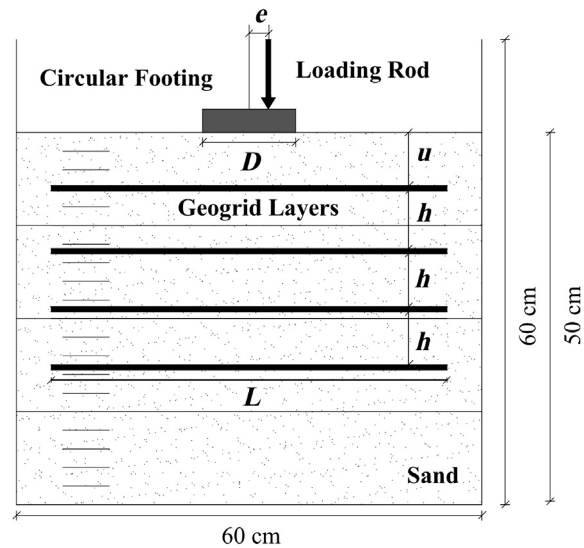

Fig. 3. Geometric parameters of geogrid reinforced sand.

footing. The tests are conducted in the displacement control condition with displacement rate of 1 mm/min. The applied displacement is continued up to the failure of soil at a settlement s about 0.25 times the footing diameter. The geometry of the reinforced sand and footing is shown in Fig. 3.

Forty five tests are carried out to study the effect of eccentric loading on a circular footing, resting on both reinforced and unreinforced sands with geogrid layers. These 45 tests consist of 5 groups of tests on a circular footing to study the effect of different load eccentricities ($e/D = 0$, 0.0625, 0.125, 0.1875 and 0.25) on load–displacement response of sand. Initially for obtaining the optimum depth ratio (u/D) for the first reinforcement layer, three tests with u/D values of 0.25, 0.42 and 0.58 are carried out. For determining the optimum depth ratio (h/D) for the second reinforcement layer, 3 tests are considered with h/D values of 0.25, 0.42 and 0.58. Three tests in unreinforced and reinforced conditions with three and four reinforcement layers are performed while the optimum values for u/D and h/D are selected for the first and second layers of geogrid to investigate the effect of number of reinforcement layers on bearing capacity. Finally, all of these 9 tests are conducted for each load eccentricity. Also, new geogrid layers are

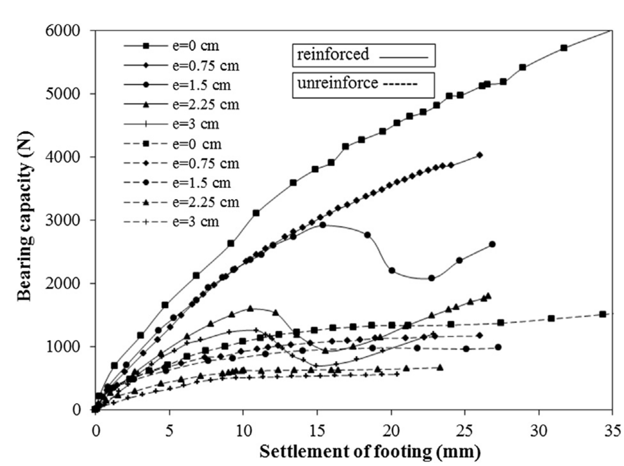

Fig. 4. Bearing capacity versus settlement of footings on reinforced and unreinforced sands with two layers at $u/D = h/D = 0.42$.

Please cite this article in press as: Badakhshan E, Noorzad A, Load eccentricity effects on behavior of circular footings reinforced with geogrid sheets, Journal of Rock Mechanics and Geotechnical Engineering (2015), http://dx.doi.org/10.1016/j.jrmge.2015.08.006

used for each test (about 80 sheets of geogrid layers are used). The load–displacement responses of the tests are verified by repeating several tests twice and the difference between the ultimate bearing capacity values is less than 2%.

4. Results and discussions

Load-settlement curves from 45 tests carried out on centrically and eccentrically loaded circular footings in both reinforced and unreinforced conditions are illustrated in Fig. 4. The ultimate bearing capacity of foundation on soil under centric and eccentric loadings has been obtained from the load-settlement curves according to suggestions made by Boushehrian and Hataf (2003) and Sawwaf (2009). In curves with an explicit peak point (for example, the curve of $e = 2.25$ cm in reinforced condition in Fig. 4), the ultimate bearing capacity and settlement at failure load are taken at the peak point.

In the present research, a dimensionless parameter, called bearing capacity ratio (*BCR*), is used to measure the effect of improvement utilizing reinforcement layers on increasing the bearing capacity. This parameter is defined as the ratio of the ultimate bearing capacity in reinforced soil to that in unreinforced soil condition (Eq. (2)). To analyze the footing settlement, the settlement ratio (*SR*) is proposed and defined as the ratio of footing settlement in reinforced soil to that in unreinforced soil condition (Eq. (3)). A new parameter called eccentric bearing capacity ratio (*EBCR*) is introduced. It can be given in form of Eq. (4) as a ratio of the ultimate load in eccentric and reinforced condition to that in centric and unreinforced condition.

$$BCR = \frac{q_{\mathrm{u(reinforced)}}}{q_{\mathrm{u(unreinforced)}}} \tag{2}$$

$$SR = \frac{s_{\mathrm{u(reinforced)}}}{s_{\mathrm{u(unreinforced)}}} \tag{3}$$

$$EBCR = \frac{q_{\mathrm{u(eccentric-reinforced)}}}{q_{\mathrm{u(centric-unreinforced)}}} \tag{4}$$

where q_u is the ultimate bearing capacity, and s_u is the footing settlement at the ultimate bearing capacity.

The ultimate bearing capacity, settlement, *BCR*, *SR* and *EBCR* for 45 tests with different eccentricities ($e = 0$ cm, 0.75 cm, 1.5 cm, 2.25 cm and 3 cm) in both unreinforced and reinforced conditions with different depth ratios are presented in Table 2.

Table 2
Results of circular footing test for $e/D = 0$, 0.0625, 0.125, 0.1875 and 0.25 in both unreinforced and reinforced sands.

e/D	Number of test	N	e (cm)	u/D	h/D	q_u (N)	s_u (mm)	BCR	SR	$EBCR$	$q_{u(eccentric)}/q_{u(centric)}$
0	1	0	0			1318	20.06	1	1		1
	2	1	0	0.25		2404	25.06	1.824	1.249	1.824	1
	3	1	0	0.42		2892	29.4	2.194	1.465	2.194	1
	4	1	0	0.58		2696	20.05	2.046	0.999	2.046	1
	5	2	0	0.42	0.25	3954	21.29	3.01	1.061	3.01	1
	6	2	0	0.42	0.42	4415	28.92	3.35	1.442	3.35	1
	7	2	0	0.42	0.58	3558	23.11	2.701	1.152	2.701	1
	8	3	0	0.42	0.42	5523	21.68	4.19	1.081	4.19	1
	9	4	0	0.42	0.42	6300	15.91	4.78	0.793	4.78	1
0.0625	10	0	0.75			1092	18.93	1	1		0.829
	11	1	0.75	0.25		2367	20.73	2.168	1.095	1.796	0.985
	12	1	0.75	0.42		2747	22.48	2.516	1.187	2.084	0.95
	13	1	0.75	0.58		1979	16.87	1.812	0.891	1.502	0.734
	14	2	0.75	0.42	0.25	3726	19.91	3.412	1.051	2.827	0.853
	15	2	0.75	0.42	0.42	3931	20.94	3.602	1.106	2.983	0.926
	16	2	0.75	0.42	0.58	3600	18.45	3.297	0.975	2.731	0.916
	17	3	0.75	0.42	0.42	4639	19.39	4.248	1.024	3.52	0.84
	18	4	0.75	0.42	0.42	4477	14.2	4.1	0.75	3.397	0.711
0.125	19	0	1.5			956	14.05	1	1		0.725
	20	1	1.5	0.25		1735	18.23	1.815	1.298	1.316	0.722
	21	1	1.5	0.42		2480	19.72	2.594	1.404	1.882	0.858
	22	1	1.5	0.58		1472	14.28	1.54	1.017	1.117	0.546
	23	2	1.5	0.42	0.25	2868	15.13	3.02	1.077	2.176	0.656
	24	2	1.5	0.42	0.42	3518	16.5	3.68	1.175	2.669	0.829
	25	2	1.5	0.42	0.58	2638	14.82	2.759	1.055	2.002	0.671
	26	3	1.5	0.42	0.42	4120	15.67	4.31	1.115	3.126	0.746
	27	4	1.5	0.42	0.42	3530	12.66	3.692	0.902	2.678	0.56
0.1875	28	0	2.25			644	8.99	1	1		0.489
	29	1	2.25	0.25		1135	15.93	1.762	1.771	0.861	0.472
	30	1	2.25	0.42		1433	15.9	2.225	1.767	1.087	0.496
	31	1	2.25	0.58		963	8.06	1.495	0.896	0.731	0.357
	32	2	2.25	0.42	0.25	1444	10.8	2.242	1.201	1.096	0.331
	33	2	2.25	0.42	0.42	1612	12.65	2.503	1.406	1.223	0.38
	34	2	2.25	0.42	0.58	1416	10.55	2.199	1.173	1.074	0.36
	35	3	2.25	0.42	0.42	2130	11.61	3.307	1.29	1.616	0.386
	36	4	2.25	0.42	0.42	1676	8.96	2.602	0.996	1.272	0.266
0.25	37	0	3			560	7.5	1	1		0.425
	38	1	3	0.25		953	11.23	1.702	1.497	0.723	0.396
	39	1	3	0.42		1201	12.2	2.145	1.627	0.911	0.415
	40	1	3	0.58		820	6.89	1.464	0.819	0.622	0.304
	41	2	3	0.42	0.25	1050	7.89	1.875	1.052	0.797	0.24
	42	2	3	0.42	0.42	1256	10.95	2.243	1.46	0.953	0.296
	43	2	3	0.42	0.58	1134	7.89	2.025	1.052	0.86	0.289
	44	3	3	0.42	0.42	1840	9.86	3.286	1.315	1.396	0.333
	45	4	3	0.42	0.42	1350	7.12	2.411	0.949	1.024	0.214

Please cite this article in press as: Badakhshan E, Noorzad A, Load eccentricity effects on behavior of circular footings reinforced with geogrid sheets, Journal of Rock Mechanics and Geotechnical Engineering (2015), http://dx.doi.org/10.1016/j.jrmge.2015.08.006

4.1. Failure mechanism

In all 45 tests, two different modes of failure, i.e. general shear failure and local shear failure, are demonstrated. In the case of general shear failure, continuous failure surfaces develop between the edges of footing and the ground surface. As the pressure increases towards the ultimate value, the soil around the edges of footing then gradually spreads downwards and outwards. Heaving of the ground surface occurs on both sides of footing. In this mode of failure, the load-settlement curve has a peak point where the ultimate bearing capacity is well defined. In the case of local shear failure, there is a significant compression of the soil under the footing. The local shear failure is characterized by the occurrence of relatively large settlements, slight heaving in surfaces and the fact that the ultimate bearing capacity is not clearly defined.

Regarding the load-settlement curves for the unreinforced and reinforced tests, it is found that the local shear failure is the mode of failure for centrically loaded footing. For the sand with 60% relative density, this is an expectation failure mode (Vesic, 1973). In eccentrically loaded footing, the failure mechanism is different in reinforced and unreinforced tests. In the tests without reinforcement layers, by increasing the load eccentricity, the mode of failure remains constant (local shear failure), whereas for the tests with reinforcement layers, the mode of failure changes by increasing the load eccentricity to general shear failure. For the tests with load eccentricity outside the footing core, the failure modes are quite the general shear failure, while for the load eccentricities inside the footing core and on the footing core boundary, it is dependent on the reinforcing conditions.

For eccentrically loaded tests in reinforced condition, the settlement continues causing strain softening to occur. Subsequently, the sand behavior changes to strain hardening and thus by increasing the settlement the corresponding load increases with an almost constant slope and geogrid layers seem to rupture. In other words, the strain hardening behavior could be attributed to the failure of geogrid sheets, because those have increased with the same slope. Strain softening is referred to as a behavior where the bearing capacity reduces with continuous development of settlement of footing (or strain of sand). Strain hardening is a process in which foundation bed is permanently deformed in order to increase resistance to further deformation.

4.2. Optimum depth of reinforcement layers

One of the important parameters in reinforced soil is the embedment depth of reinforcement layers from the soil surface. The optimum spacing of reinforcement layers is studied experimentally in this section. According to previous studies, several findings were reported for u and h in centric loading condition. Researchers emphasized that there is critical values for u and h beyond which further increase has not any effect on bearing capacity. Boushehrian and Hataf (2003), Mosallanezhad et al. (2008), and Latha and Somwanshi (2009) have shown through the tests on circular and square footings that the optimum depth of the first reinforcement layer and the vertical spacing between reinforcement layers that provide the maximum *BCR* vary from 0.2 to 0.5 for u/D or u/B and from 0.3 to 0.6 for h/D or h/B, respectively. For centrically and eccentrically loaded footings, three different depths including 3 cm, 5 cm and 7 cm from footing bottom are considered for the first and second layers of geogrid (in dimensionless condition $u/D = 0.25$, 0.42 and 0.58 and $h/D = 0.25$, 0.42 and 0.58 are considered). The results for embedment depth ratios of the first layer of reinforcement versus the *BCR* are shown in Fig. 5. As is obvious in this figure, the depth ratio of $u/D = 0.42$ gives the highest *BCR* at all load eccentricities. For the second layer of reinforcement,

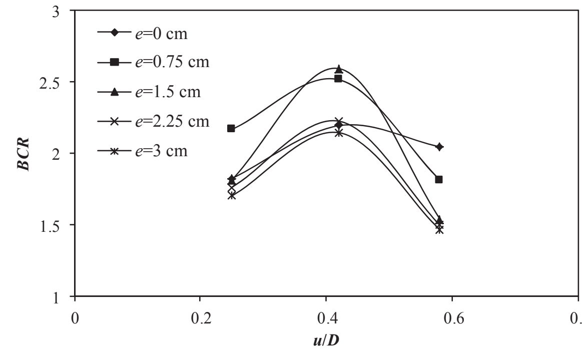

Fig. 5. Variations of *BCR* with u/D ratio for the first layer of reinforcement.

different depth ratios including $h/D = 0.25$, 0.42 and 0.58 are considered to determine the optimum value of h/D by maintaining $u/D = 0.42$ as a constant. Results of h/D changing with the *BCR* are shown in Fig. 6 for both centric and eccentric loadings. It can be seen from this figure that, for depth ratio of $h/D = 0.42$, the maximum *BCR* has occurred. Thus, the optimum value for u and h in all tests can be considered to be about 5 cm (equal to $u/D = h/D = 0.42$). Consequently, for the tests with more than 2 layers of reinforcement, the embedment depth ratio is chosen as 0.42.

4.3. Effect of number of geogrid layers

Several tests are carried out with the same depth ratio ($u/D = h/D = 0.42$) to find out the effect of number of geogrid layers on *BCR* for centrically loaded circular footing and different load eccentricities ($e = 0.75$ cm, 1.5 cm, 2.25 cm and 3 cm). The number of geogrid layers (N) is assumed from 1 to 4. The *BCR* versus N is plotted in Fig. 7. It is revealed that the *BCR* in centrically loaded footing

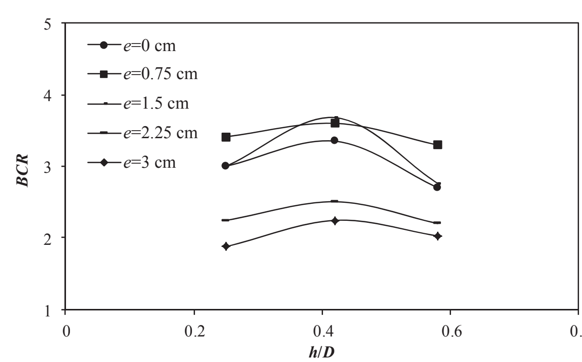

Fig. 6. Variations of *BCR* with h/D ratio for the second layer of reinforcement.

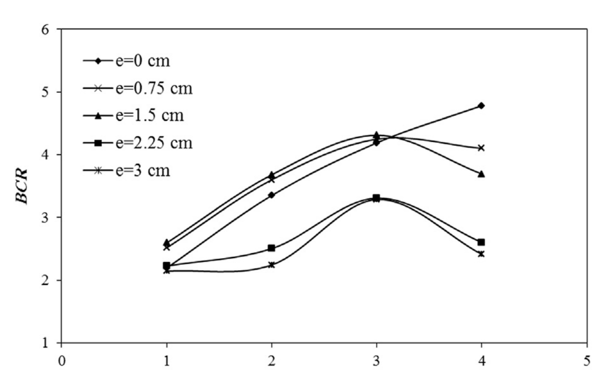

Fig. 7. Variations of *BCR* with N for centric and eccentric loadings.

increases by increasing N to 4 layers of geogrid. This finding was reported previously by Boushehrian and Hataf (2003) proposing that, for N greater than 4, the effect of geogrid layers is negligible. However, optimum number of reinforcement layers is dependent on embedment depth ratio of reinforcement, and in centric loading condition, the BCR increases to 4.19 at 3 layers of geogrid with $u/D = h/D = 0.42$. Nevertheless, in centric loading condition, the 4th layer of reinforcement increases the BCR to 4.78, but in eccentric loading condition, the BCR increases at 3 layers of reinforcement and the 4th layer of geogrid has a reducing effect. Sawwaf (2009) obtained the same conclusion for strip footing and Sawwaf and Nazir (2012) reported that $N = 3$ is the optimum number of geogrid layers in eccentric loading condition for ring footing over geogrid reinforced sand and beyond $N = 3$ the effect of reinforcement layers on the bearing capacity ratio can be neglected. In addition, the effective depth under the circular footing in eccentric loading condition is influenced by two elements. The effective depth has been reduced with increasing load eccentricity. On the other hand, the reduction of footing settlement at the ultimate load occurs with increasing number of geogrid layers. The photographs of geogrid sheets before and after the testing are shown in Fig. 8. After the loading of each test (at the end of each test), the diameter of punching rupture on each geogrid sheet is measured. As shown in Fig. 8, the small punching and large punching are related to lower and upper layers of geogrids, respectively. Consequently, the failure mechanisms are predicted.

According to Fig. 9, when 4 layers of reinforcement are used, the failure wedge cannot develop into a larger depth in comparison with those cases with three layers of reinforcement. As a result, the ultimate bearing capacity has been decreased in comparison with a case with 3 layers of reinforcement. In the condition of centric loading, similar results were stated by Yetimuglu et al. (1994), Adams and Collin (1997), and Boushehrian and Hataf (2003). To conclude this section, by increasing the number of reinforcement layers from an optimum number, the BCR tends to decrease due to lateral slipping of sand particles on reinforcement layers.

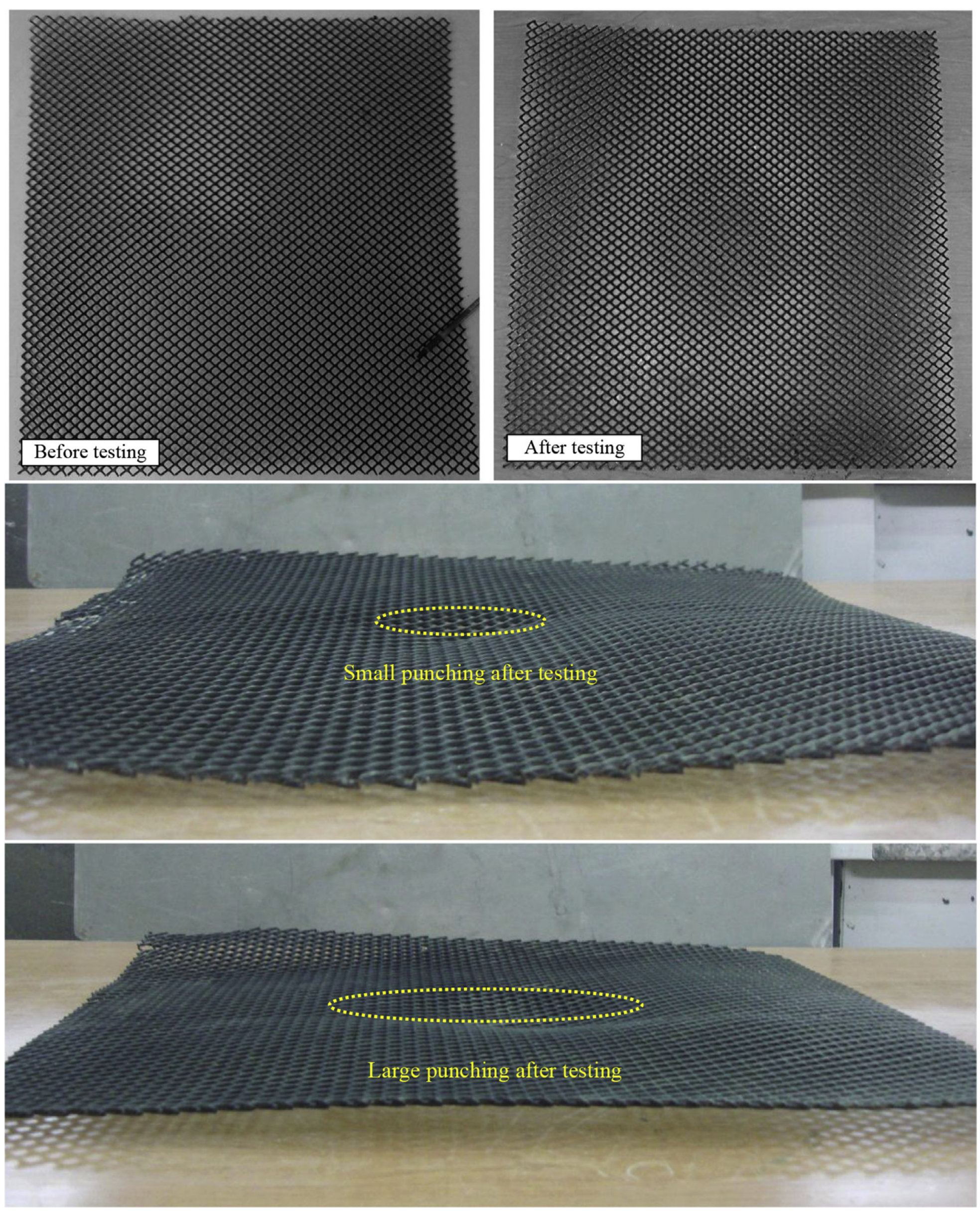

Fig. 8. The photographs of geogrid sheets before and after testing.

Please cite this article in press as: Badakhshan E, Noorzad A, Load eccentricity effects on behavior of circular footings reinforced with geogrid sheets, Journal of Rock Mechanics and Geotechnical Engineering (2015), http://dx.doi.org/10.1016/j.jrmge.2015.08.006

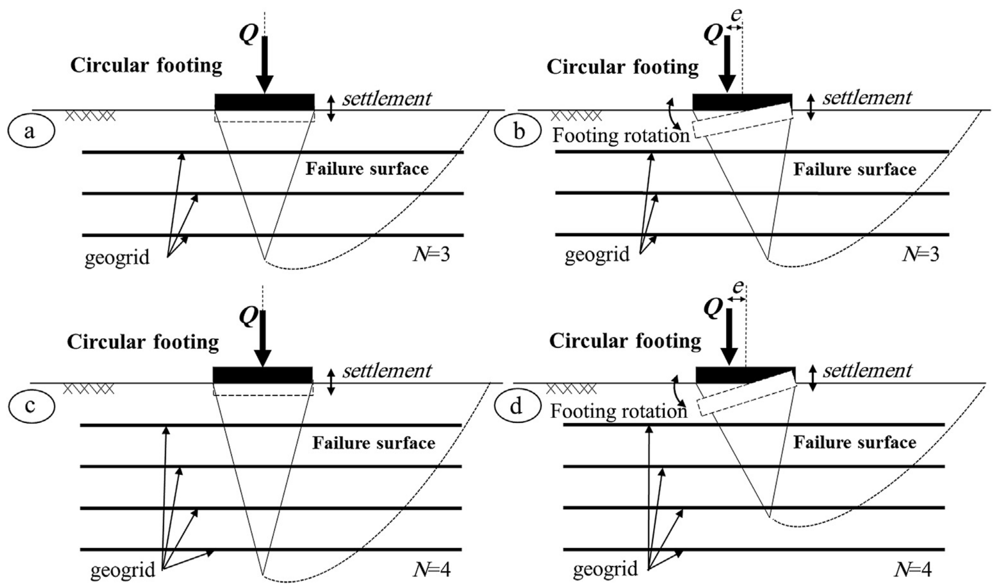

Fig. 9. Failure mechanisms for three and four layers of geogrid under centric and eccentric loadings. (a) $N = 3$ and centrically loaded. (b) $N = 3$ and eccentrically loaded. (c) $N = 4$ and centrically loaded. (d) $N = 4$ and eccentrically loaded.

4.4. Effect of load eccentricity on bearing capacity

In order to investigate the effect of load eccentricity on both unreinforced and reinforced sands for circular footing, different load eccentricities are considered. Results indicate that the ultimate bearing capacity decreases with increasing load eccentricity in both unreinforced and reinforced sands with geogrid layers. By increasing the load eccentricity, the decrease rate of ultimate bearing capacity in unreinforced condition is much lower than that in reinforced condition. When reinforcements are placed in an optimum distance from the footing bottom ($u/D = h/D = 0.42$), the decrease rates of ultimate bearing capacity at a load eccentricity to the core boundary of footing ($e = 0.75$ cm and 1.5 cm) are less than those in unreinforced condition. Further, by increasing load eccentricity away from the core boundary of footing ($e = 2.25$ cm and 3 cm), the decrease in ultimate bearing capacity is greater than that in unreinforced condition. The bearing capacity ratio (*BCR*) versus the load eccentricity for one to four layers of geogrid is shown in Fig. 10. When reinforcement layer is placed in an optimum depth, the effect of geogrid layers on bearing capacity increases by increasing the load eccentricity to the core boundary of footing ($e = 1.5$ cm). The *BCR* decreases significantly at greater load eccentricity from the core boundary of footing and by increasing the load eccentricity further outside the core, the contribution of reinforcement becomes much lower or negligible. This increase in *BCR* for eccentrically loaded circular footing, in comparison with centrically loaded circular footing, is previously shown in a test by Sadoglu et al. (2009) for strip footing on geotextile reinforced sand. Similar conclusion was also reported by Sawwaf and Nazir (2012) for eccentrically loaded ring footing on reinforced layered soil that *BCR* increases considerably to a value of $e/D_0 = 0.15$ (D_0 is the diameter of ring footing), after which the increase rate of the *BCR* becomes much lower. It is also clearly observed that, by increasing the number of reinforcement layers from one layer (Fig. 10a) to three layers (Fig. 10c), the *BCR* increases, and for four layers of reinforcement it is lower than that in the case of three layers.

From Table 2, it is realized that, by increasing the load eccentricity, the ultimate bearing capacity occurs at lower settlement. However, when the sand bed is reinforced with geogrid layers, a larger settlement is necessary in comparison with unreinforced

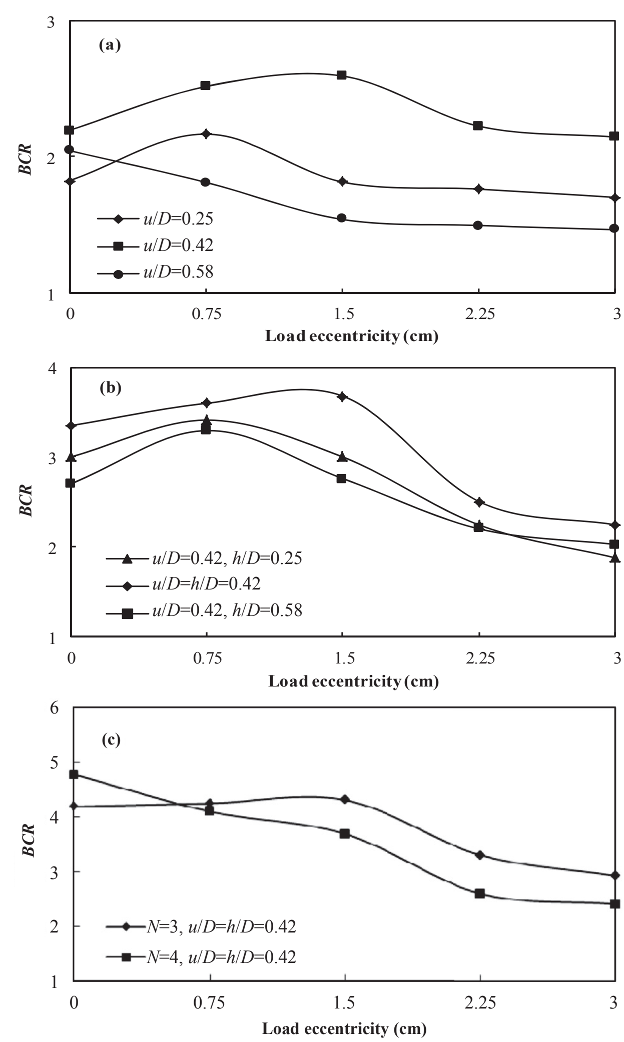

Fig. 10. Variations of *BCR* with *e* for (a) one layer, (b) two layers, (c) three and four layers of reinforcement.

Please cite this article in press as: Badakhshan E, Noorzad A, Load eccentricity effects on behavior of circular footings reinforced with geogrid sheets, Journal of Rock Mechanics and Geotechnical Engineering (2015), http://dx.doi.org/10.1016/j.jrmge.2015.08.006

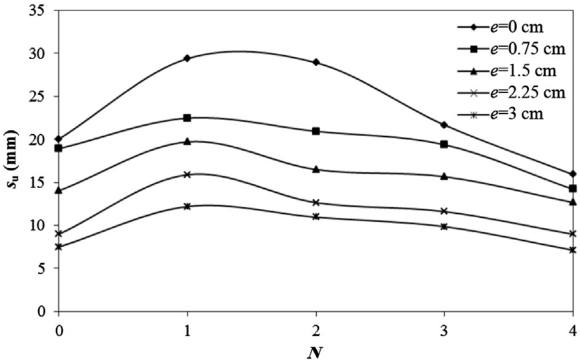

Fig. 11. Variations of s_u with number of geogrid layers for centric and eccentric loadings.

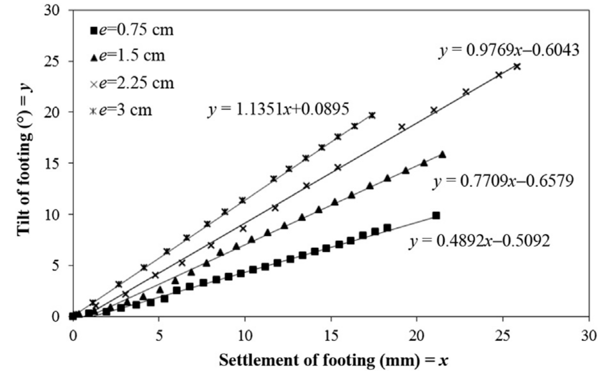

Fig. 12. Tilt of footing versus settlement for each load eccentricity for one layer geogrid at $u/D = 0.58$.

condition. Use of geogrid layers causes the footing settlement corresponding to the constant load intensity to reduce. From the factor *SR*, it can be concluded that the settlement at the ultimate bearing capacity for centrically loaded circular footing without reinforcement layers is larger than that of eccentrically loaded circular footing in reinforced condition. The settlements at the ultimate bearing capacity, s_u, versus the number of geogrid layers, *N*, for different load eccentricities are shown in Fig. 11. This figure clearly indicates that, in the same condition of load eccentricity, the settlement at the ultimate load decreases by increasing the number of geogrid layers and it occurs mostly in one layer of geogrid. The results indicate that reduction rate of settlement at the ultimate bearing capacity decreases with increasing load eccentricity.

When the reinforcement layers are located in optimum values ($u/D = h/D = 0.42$), the ultimate bearing capacity for each load eccentricity (inside and outside the footing core) has a larger quantity than centric and unreinforced bearing capacity. It is worth noting that using reinforcement layers ensures the ultimate bearing capacity of circular foundation designed regardless of eccentric loading. For sudden natural eccentric loads exerted on the foundation, no bearing capacity reduction is applied when compared to the initial state (unreinforced and regardless of load eccentricity).

The factor $q_{u(eccentric)}/q_{u(centric)}$ is also computed for both unreinforced and reinforced conditions which is given in Table 2. It can be concluded that, by increasing the load eccentricity, this factor decreases. Thus, when the geogrid layers are placed in optimum depth ($u/D = h/D = 0.42$) for the load eccentricities inside the footing core, this factor is larger than that in unreinforced condition and for the load eccentricities outside the footing core for unreinforced condition it is larger than that in reinforced condition.

4.5. Tilt of footing

When a footing is subjected to eccentric loading, footing tilt is inevitable. The effect of geogrid layers on the behavior of circular footing tilt, as an unknown issue, is investigated prior to recognition of the effect of geogrid layers on the *BCR* for eccentrically loaded circular footing. In this study, in order to calculate the tilt of circular footing, two LVDTs are used for measuring the settlement of footing in two different places: one LVDT on loading rod and one LVDT on surface of footing in a certain location along the load eccentricity. The tilt of footing is calculated with respect to the difference of settlement of footing recorded by two LVDTs. For each test, with eccentric loading the tilt of footing is measured. The tilt of footing versus the settlement of footing is shown in Fig. 12 for one layer of geogrid with depth ratio of $u/D = 0.58$ for all load eccentricities. From the tilt-settlement curves in both reinforced and

Table 3
Rates of circular footing tilt for different load eccentricities.

Test condition	N	A			
		$e = 0.75$ cm	$e = 1.5$ cm	$e = 2.25$ cm	$e = 3$ cm
Unreinforced	0	0.681	0.865	0.983	1.155
$u/D = 0.25$	1	0.421	0.644	1.153	1.23
$u/D = 0.42$	1	0.411	0.61	0.802	0.985
$u/D = 0.58$	1	0.489	0.771	0.977	1.135
$u/D = 0.42$, $h/D = 0.25$	2	0.447	0.715	0.849	1.052
$u/D = h/D = 0.42$	2	0.356	0.589	0.723	0.903
$u/D = 0.42$, $h/D = 0.58$	2	0.494	0.706	0.831	0.99
$u/D = h/D = 0.42$	3	0.454	0.682	0.845	0.994
$u/D = h/D = 0.42$	4	0.789	0.941	1.164	1.321

unreinforced cases, it is found that the tilt of footing increases with increasing footing settlement linearly. It is clear that the tilt of footing is not corresponding to the failure of soil under footing and, thus, the tilt of footing before and after failure has a constant increase rate. As shown in Fig. 12, a trend line is plotted for each tilt-settlement response equal to $y = Ax + B$, where *A* is the rate of footing tilt, and *B* is the constant of tilt rate. The quantities of *A* for every test are measured and summarized in Table 3. The maximum variation of *B* is computed to be ± 0.5 which is negligible and does not have any main effect on the tilt computations. As is expected, it is seen in Table 3 that, by increasing the load eccentricity, the tilt of footing for the constant reinforced condition increases with increasing load eccentricity.

Fig. 13 shows that, by increasing the load eccentricity, the tilt of circular footing increases with a constant ratio of about 0.2353. Consequently, when the tilt of footing for a test is specified (with each reinforced condition), the tilt of footing for any load eccentricity (all variables are constant except for the load eccentricity) can be measured by this quantity (*A*). The other conclusion revealed

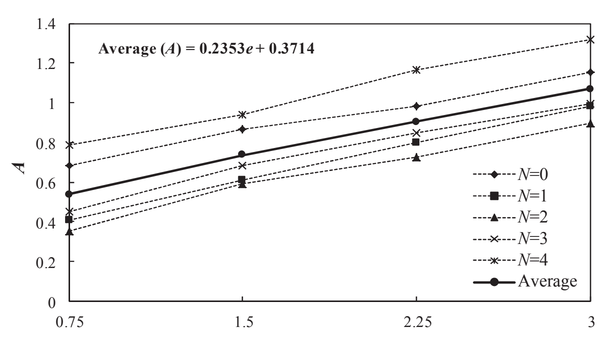

Fig. 13. Variations of *A* with load eccentricity in both unreinforced and reinforced tests.

Please cite this article in press as: Badakhshan E, Noorzad A, Load eccentricity effects on behavior of circular footings reinforced with geogrid sheets, Journal of Rock Mechanics and Geotechnical Engineering (2015), http://dx.doi.org/10.1016/j.jrmge.2015.08.006

from Table 3 is that the rate of the footing tilt under the geogrid depth ratios of $u/D = 0.42$ and $h/D = 0.42$ at 2 layers is the minimum in comparison with two other depth ratios of u/D and h/D, i.e. 0.25 and 0.58, respectively. In addition to the maximum *BCR*, the minimum tilt rate has occurred in reinforcement depth ratio of $u/D = h/D = 0.42$ for all load eccentricities. It is also observed that the tilt of footing decreases by increasing the number of reinforcement layers to 2 layers, afterwards the tilt rate increases. This trend is perceived for all load eccentricities (inside and outside the footing core).

5. Conclusions

The behaviors of eccentrically loaded circular footing supported on both unreinforced and reinforced sands with geogrid layers are studied based on a series of tests. Load eccentricities are considered with different values (e = 0.75 cm, 1.5 cm, 2.25 cm and 3 cm) in order to understand the effect of geogrid reinforcement layers on the bearing capacity, settlement and tilt for load eccentricity inside and outside the footing core boundary. The following conclusions can be drawn from this study:

(1) The maximum bearing capacity for centric and eccentric loadings on reinforced sand bed occurs at the distance of $u/D = 0.42$ between the first layer of geogrid and base of footing. The optimum vertical distance between other geogrid layers is $h = 0.42D$. For eccentrically loaded circular footing, the bearing capacity increases at 3 layers of reinforcement, beyond which the reinforcement layers do not contribute to any improvement effects.
(2) The failure mechanism for reinforced and unreinforced sands in centrically loaded circular footing is local shear failure, while by increasing the load eccentricity it tends to approach general shear failure in reinforced condition.
(3) The *BCR* increases with increasing number of geogrid layers, and when reinforcement layers are placed in optimum depth, the *BCR* increases with increasing load eccentricity to the footing core boundary, beyond which the *BCR* can be decreased.
(4) Based on the results of this study, the ultimate bearing capacity under eccentric loading occurs in a lower settlement in comparison with centric loading in both unreinforced and reinforced conditions. With increasing number of geogrid layers, the settlement increases considerably initially (about 1 layer) and afterwards decreases.
(5) The rate of tilt (A) increases by increasing the load eccentricity linearly, and with the increase in number of geogrid layers, the rate of tilt decreases at 2 layers of reinforcement.

It should be noted that the results demonstrated in this paper are related to the circular footing with diameter of 12 cm on sand bed and limited to this sand type, density and loading rate selection conditions and that effects of some other parameters such as scale effect, density of soil, diameter of footing, embedment depth of footing, etc. have not been investigated herein.

Conflict of interest

The authors confirm that there are no known conflicts of interest associated with this publication and there has been no significant financial support for this work that could have influenced its outcome.

References

Adams M, Collin J. Large model spread footing load tests on geosynthetic reinforced soil foundations. Journal of Geotechnical and Geoenvironmental Engineering 1997;123(1):66–72.

Alawaji HA. Settlement and bearing capacity of geogrid-reinforced sand over collapsible soil. Geotextiles and Geomembranes 2001;19(2):75–88.

Al-Tirkity J, Al-Taay A. Bearing capacity of eccentrically loaded strip footing on geogrid reinforced sand. Journal of Engineering Sciences 2012;19(1):14–22.

ASTM D422-90. Standard test method for particle-size analysis. West Conshohocken, PA, USA: ASTM International; 1990.

Basudhar PK, Saha S, Deb K. Circular footings resting on geotextile-reinforced sand bed. Geotextiles and Geomembranes 2007;25(6):377–84.

Boushehrian J, Hataf N. Experimental and numerical investigation of the bearing capacity of model circular and ring footing on reinforced sand. Geotextiles and Geomembranes 2003;21(4):241–56.

Dhillon GS. Settlement, tilt and bearing capacity of footings under central and eccentric loads. Journal of the National Building Organisation 1961;6(2):66–78.

Eastwood W. The bearing capacity of eccentrically loaded foundations on sandy soil. Structural Engineer 1955;33(6):181–7.

Ghosh A, Ghosh A, Bera AK. Bearing capacity of square footing on pond ash reinforced with jute-geotextile. Geotextiles and Geomembranes 2005;23(2):144–73.

Graudet P, Kerisel J. Recherges experimentation sur les foundations soumises des effort inclines au exentres. Annales des Ponts et Chauses 1965;13(3):167–93 (in French).

Highter WH, Anders JC. Dimensioning footings subjected to eccentric loads. Journal of Geotechnical Engineering 1985;111(5):659–63.

Kumar A, Ohri ML, Bansal RK. Bearing capacity tests of strip footings on reinforced layered soil. Geotechnical and Geological Engineering 2007;25(2):139–50.

Latha M, Somwanshi A. Effect of reinforcement form on the bearing capacity of square footings on sand. Geotextiles and Geomembranes 2009;27(6):409–22.

Lee IK. Foundations subjected to moments. In: Proceedings of the 6th International Conference on Soil Mechanics and Foundation Engineering; 1965. p. 108–12.

Lovisa J, Shukla SK, Sivakugan N. Behavior of prestressed geotextile-reinforced sand bed supporting a loaded circular footing. Geotextiles and Geomembranes 2010;28(1):23–32.

Mahiyar H, Patel AN. Analysis of angle shaped footing under eccentric loading. Journal of Geotechnical and Geoenvironmental Engineering 2000;126(12):1151–6.

Meyerhof GG. The bearing capacity of foundations under eccentric and inclined loads. In: Proceedings of the 1st Conference on Soil Mechanics and Foundation Engineering; 1953. p. 440–9.

Michalowski R, You L. Effective width rule in calculations of bearing capacity of shallow footings. Computers and Geotechnics 1998;23(4):237–53.

Moghaddas Tafreshi SN, Dawson AR. Comparison of bearing capacity of a strip footing on sand with geocell and with planar forms of geotextile reinforcement. Geotextiles and Geomembranes 2010;28(1):72–84.

Mosallanezhad M, Hataf N, Ghahramani A. Experimental study of bearing capacity of granular soils reinforced with innovative grid-anchor system. Geotechnical and Geological Engineering 2008;26(3):299–312.

Prakash S, Saran S. Bearing capacity of eccentrically loaded footings. Journal of the Soil Mechanics and Foundations Division, ASCE 1971;97(1):95–103.

Patra CR, Das BM, Bhoi M, Shin EC. Eccentrically loaded strip foundation on geogrid-reinforced sand. Geotextiles and Geomembranes 2006;24(4):254–9.

Purkayastha RD, Char RAN. Stability analysis for eccentrically loaded footings. Journal of Geotechnical Engineering Division, ASCE 1977;103(6):647–53.

Sadoglu E, Cure E, Moroglu B, Uzuner BA. Ultimate loads for eccentrically loaded model shallow strip footings on geotextile-reinforced sand. Geotextiles and Geomembranes 2009;27(3):176–82.

Sawwaf M. Experimental and numerical study of eccentrically loaded strip footings resting on reinforced sand. Journal of Geotechnical and Geoenvironmental Engineering 2009;135(10):1509–18.

Sawwaf ME, Nazir A. Behavior of eccentrically loaded small-scale ring footings resting on reinforced layered soil. Journal of Geotechnical and Geoenvironmental Engineering 2012;138(3):376–84.

Sitharam TG, Sireesh S. Model studies of embedded circular footing on geogrid-reinforced sand beds. Ground Improvement 2004;8(2):69–75.

Taiebat HA, Carter JP. Bearing capacity of strip and circular foundations on undrained clay subjected to eccentric loads. Géotechnique 2002;52(1):61–4.

Vesic AS. Analysis of ultimate loads of shallow foundations. Journal of Soil Mechanics and Foundation Engineering Division, ASCE 1973;99(1):45–55.

Vinod P, Bhaskar AB, Sreehari S. Behavior of a square model footing on loose sand reinforced with braided coir rope. Geotextiles and Geomembranes 2009;27(6):464–74.

Yetimuglu T, Wu JTH, Saglamar A. Bearing capacity of rectangular footings on geogrid-reinforced sand. Journal of Geotechnical Engineering, ASCE 1994;120(12):2083–99.

Ali Noorzad obtained a Ph.D. degree from Concordia College, Canada in 1998 working on cyclic behavior of cohessionless granular media using the compact state concept. He is a professor in Faculty of Civil, Water & Environmental Engineering, Shahid Beheshti University in Tehran. His research interests include plasticity concepts and constitutive modeling, finite element simulations, soil dynamics and ground improvement.

Please cite this article in press as: Badakhshan E, Noorzad A, Load eccentricity effects on behavior of circular footings reinforced with geogrid sheets, Journal of Rock Mechanics and Geotechnical Engineering (2015), http://dx.doi.org/10.1016/j.jrmge.2015.08.006